materials

MDPI

Article

Swelling Pressure of Selected Tropical Hardwoods and Plantation-Grown Paulownia

Przemysław Mania *, Miłosz Stasiak, Franciszek Choja and Magdalena Broda *

Department of Wood Science and Thermal Techniques, Faculty of Forestry and Wood Technology, Poznan University of Life Sciences, ul. Wojska Polskiego 38/42, 60-637 Poznan, Poland
* Correspondence: przemyslaw.mania@up.poznan.pl (P.M.); magdalena.broda@up.poznan.pl (M.B.)

Highlights

- Maximum swelling pressure varied significantly among species (1.17–8.85 MPa), with the highest values in sapele and the lowest in paulownia.
- Swelling pressure anisotropy and development rates were species-dependent, whereas density and stiffness alone did not fully account for the observed differences.
- Species-specific swelling pressure and the anatomical direction of swelling should be considered when selecting wood for applications involving restrained moisture-induced expansion.
- The findings provide a basis for improving the design and durability of wood products and connections exposed to moisture variations.

Abstract

Wood is a hygroscopic material, and water uptake causes dimensional changes associated with swelling. When swelling is restrained, internal stresses and swelling pressure develop, which may contribute to cracking, deformation and damage to wood elements. Knowledge of swelling pressure is therefore important for assessing the dimensional stability and appropriate application of exotic wood, particularly under variable humidity conditions. Unfortunately, comparative data for swelling pressure of tropical hardwoods and plantation-grown paulownia remain limited. Therefore, this study examined the magnitude, anisotropy, and time-dependent development of swelling pressure in sapele, khaya, framiré, tauari, abura, mansonia, and paulownia wood submerged in water while the wood was restrained from swelling. Six replicates of each wood species in each direction were examined. Maximum tangential and radial pressures were measured and related to wood density and compressive modulus of elasticity (MOE). Swelling pressure was measured from oven-dry starting conditions until the maximum swelling pressure was reached, as indicated by stabilisation or a decrease in the measured force. Maximum swelling pressure ranged from 1.81 to 7.00 MPa tangentially and from 1.17 to 8.85 MPa radially. Sapele exhibited the highest pressures in both directions (7.00 and 8.85 MPa), whereas paulownia showed the lowest (1.81 and 1.17 MPa). Pressure development differed among species: paulownia, abura, and mansonia reached comparatively low maxima rapidly, while sapele and khaya developed higher pressures more slowly. Tauari combined rapid initial development with a high maximum pressure. Following their maxima, pressures declined slightly. Swelling pressure increased significantly with wood density in both tangential ($R^2 = 0.68$) and radial ($R^2 = 0.62$) directions. Its relationship with MOE was significant tangentially ($R^2 = 0.61$), but not radially. Substantial differences

Academic Editor: Philippe Evon

Received: 16 October 2026
Revised: 9 November 2026
Accepted: 10 November 2026
Published: 12 November 2026

Copyright: © 2026 by the authors. Licensee MDPI, Basel, Switzerland. This article is an open access article distributed under the terms and conditions of the Creative Commons Attribution (CC BY) license.

among species of similar density demonstrate that density and stiffness alone cannot reliably predict swelling pressure. The results indicate that swelling pressure is governed by a combination of species-specific characteristics, anatomical direction, and time-dependent behaviour, with wood density and compressive stiffness providing only partial explanations for the observed variability. These wood features need to be considered while designing moisture-exposed, dimensionally constrained wood products. Further research focusing on the detailed characterisation of wood anatomy and moisture transport properties is necessary to clarify the mechanisms responsible for differences in swelling pressure between species and anatomical directions, and to improve prediction under restrained moisture-induced swelling conditions.

Keywords: tropical wood; abura; sapele; khaya; mahogany; wood swelling

1. Introduction

Wood is a hygroscopic material that absorbs and releases moisture in response to changes in the surrounding environment. Moisture uptake causes changes in wood dimensions (swelling), particularly in the radial and tangential directions. These changes depend on the anatomical structure of wood, its chemical composition, and the conditions of moisture exposure [1].

Wood swelling is defined as an increase in its dimensions resulting from the absorption of bound water into the cell walls [1,2]. When this moisture-induced dimensional expansion is completely restrained, internal stresses develop. The stress required to prevent such deformation is referred to as swelling pressure and represents the maximum stress generated under restrained swelling conditions [3–5]. The pressure developed when a material absorbs moisture from the oven-dry state up to the fibre saturation point is defined as total swelling pressure [6]. Particularly high swelling pressures may occur when initially dry wood is fully restrained before exposure to water [4,7]. It is important to distinguish between swelling pressure and free swelling. Free swelling describes the dimensional changes in wood without external restraint, whereas swelling pressure represents the stress generated when expansion is restricted. Therefore, measurements of shrinkage or swelling coefficients alone are insufficient to determine the mechanical forces that wood may exert on surrounding elements under humid conditions [5,8].

The ability of wood to generate considerable forces during moisture absorption has been exploited in practical applications. It is believed that ancient Egyptians used this phenomenon to extract stone blocks from rock formations. Dry wooden pegs were inserted into holes drilled in the rock and then wetted, causing the wood to expand and generate sufficient pressure to separate the stone blocks from the rock surface [9,10]. A similar principle is applied in woodworking and joinery, where wooden components may be oven-dried before assembly. Subsequent moisture absorption from the surrounding air causes the wood to swell, increasing the tightness and strength of the resulting joints [11]. The potential use of moisture-induced swelling to improve the performance of wooden connections has also been investigated experimentally on densified beech wood for application as a swelling dowel in timber joints [11].

Despite these beneficial applications, swelling and the associated pressure are generally considered undesirable in the industrial use of wood, where wood elements are often connected to other components, bonded with adhesives, or installed with limited space for expansion. Under these conditions, moisture-induced swelling can generate mechanical stresses that can damage both wood-based products and adjacent materials or

structural elements [5,12]. Therefore, both dimensional stability and swelling pressure are important properties for evaluating the performance of wood products exposed to elevated relative humidity. Understanding moisture-induced swelling, stress development, and subsequent stress relaxation is essential for predicting and limiting deformation and cracking, thereby improving the durability and extending the service life of wood and wood-based products [12].

Investigation of swelling pressure is particularly important in industrial applications where wood expansion is partially or fully restricted. Therefore, for this study, several tropical wood species and plantation-grown paulownia used for flooring, joinery, garden furniture, decking, door and window frames, plywood and other products, where dimensional stability is important, were selected, including sapele (*Entadrophragma cylindricum* Sprague), African mahogany (*Khaya ivorensis* A. Chev.), framiré (*Terminalia ivorensis* A, Chev.), tauari (*Couratari tauari*), abura (*Hallea ciliata* P.), mansonia (*Mansonia altissima* A. Chev.), and paulownia (*Paulownia tomentonsa* (Thunb.) Steud.).

Sapele (*Entandrophragma cylindricum*) is a medium-heavy tropical hardwood originating from the tropical forests of West and Central Africa, valued for its suitability in structural and carpentry applications, as well as for its common use in the production of artistic and decorative objects. It is also used in the manufacture of furniture and flooring products, and as decorative face layers of multilayer flooring materials [13–15]. It has a diffuse-porous structure, often with distinct growth-ring boundaries, banded axial parenchyma, multiseriate rays, and vessels containing tyloses [16–18]. Its dry density ranges from 560 to 780 kg/m^3, with typical values of 640–690 kg/m^3. The modulus of elasticity (MOE) is approximately 10–14 GPa, while the modulus of rupture (MOR) ranges from 99 to 121 MPa [16,18–20]. Sapele is relatively sensitive to moisture changes, showing higher hygroscopicity, shrinkage, and swelling than other related *Entandrophragma* species, particularly at higher temperatures. Radial and tangential shrinkage are approximately 4.8% and 7.2%, respectively, with volumetric shrinkage of 12.8% and a tangential-to-radial (T/R) shrinkage ratio of 1.5. Its anatomical organisation strongly influences both structural integrity and lateral mechanical response [19,21–23].

African mahogany (*Khaya ivorensis*), referred to for short as khaya throughout the manuscript, is a low- to medium-density tropical hardwood native to the lowland tropical rainforests and moist forests of West and Central Africa. Its wood is primarily valued for its warm reddish-brown colour, good dimensional stability, and excellent workability. It is suitable for making furniture, interior finishing, flooring, boat components, and decorative veneers for plywood, and is frequently used as an accessible substitute for true mahogany [24–27]. It has a diffuse-porous structure with weakly defined growth rings, mostly solitary vessels or short radial multiples, multiseriate rays, vessels occasionally filled with brownish deposits (gum or resin), and frequently septate fibres [27–30]. Its density typically ranges from 500 to 570 kg/m^3, with an average of approximately 530 kg/m^3. The MOE ranges from 6.7 to 10.0 GPa, while the MOR is approximately 54–79 MPa [28,31–33]. The wood shows relatively good dimensional stability, with radial shrinkage of approximately 4.2%, tangential shrinkage of 5.7%, and volumetric shrinkage of about 10%, resulting in a T/R ratio of 1.4. It is generally less prone to twisting, cupping, and checking during drying than many other commercial hardwoods. However, end splitting may occur, and its physical and mechanical properties vary with anatomical structure and radial position within the stem [23,25,31,34,35].

Framiré (*Terminalia ivorensis*) is a moderately lightweight tropical hardwood originating from moist tropical rainforests and seasonal forests of West Africa. Its wood is used as solid timber in building and construction applications, in joinery, door and window frames, furniture and plywood [26,36,37]. It has a diffuse-porous structure with predominantly solitary vessels, occasional short groups of vessels, tyloses, and non-

storied rays. Its anatomical properties vary between juvenile and mature wood and between different parts of the tree [38–40]. The density of stemwood and branchwood typically ranges from 490 to 540 kg/m^3. Its mechanical properties are moderate, with an MOR of approximately 71 MPa and an MOE of 7.0–9.3 GPa [41–44]. However, across the tree, anatomical proportions directly drive engineering performance: stemwood exhibits greater fibre and vessel volume fractions and longer fibres than branchwood, conferring superior longitudinal load-bearing capacity, while branchwood shows higher compression and shear parallel to the grain, as well as a slightly elevated MOR of 73 MPa [39,41,45]. Framiré shows relatively low shrinkage, with radial and tangential values of approximately 3.5% and 5.2%, respectively, and volumetric shrinkage of about 9.0–9.3%. The T/R shrinkage ratio is approximately 1.5. The wood dries rapidly, with limited splitting, twisting, and distortion [41]. In service, despite its moderate density, framiré demonstrates exceptional natural termite resistance [43]. However, it exhibits time-dependent creep and mechano-sorptive effects that necessitate reliability-based consideration under changing environmental conditions [44,46].

Tauari (*Couratari tauari*) is a moderately heavy tropical hardwood native to the Amazon Basin with a specific, quite unpleasant, linen-like smell. It is used in flooring, construction components (including frames, ceilings, wall panelling), furniture, and interior finishing [47,48]. It has a diffuse-porous structure with predominantly solitary vessels, short radial vessel multiples, narrow bands of axial parenchyma, and non-storied rays. Silica bodies and prismatic crystals are common and may cause tool wear during processing [49,50]. Its basic density ranges from approximately 500 to 680 kg/m^3, while the apparent density is about 740–820 kg/m^3. Mechanically, clear timber exhibits moderate stiffness and load-bearing performance compatible with light structural framing, carpentry, and joinery. The MOE ranges from 10.1 to 14.0 GPa, and the MOR from 90 to 118 MPa [47,50–54]. Tauari displays good dimensional stability in service. Radial and tangential shrinkage are approximately 4.5% and 7.0%, respectively, with a volumetric shrinkage of 11–13%. The T/R shrinkage ratio is approximately 1.6, indicating relatively pronounced shrinkage anisotropy. It is classified as a low-natural-durability timber, susceptible to wood-decaying fungi and subterranean termites unless thermally modified or vacuum-impregnated with preservatives [47,54,55]. The species is generally very little known compared to the rest of the study.

Abura (*Hallea ciliata*) is a moderately lightweight tropical hardwood native to freshwater swamp forests of West and Central Africa. The wood is used in furniture manufacturing, interior joinery, particleboard, veneer and plywood production. Its potential as a raw material for binderless wood-based panels has also been demonstrated experimentally [37,56,57]. It has a diffuse-porous structure, predominantly solitary vessels, and a relatively uniform texture. The sapwood and heartwood are not clearly differentiated [58,59]. Its average density is approximately 540 kg/m^3, with values around 560 kg/m^3 reported for dried wood. The MOR is approximately 81.1 MPa, while the MOE ranges from 8.8 to 12.6 GPa. The wood dries rapidly and is relatively easy to process. However, it has low natural resistance to fungal decay and wood-destroying insects, particularly subterranean termites [43,58].

Mansonia (*Mansonia altissima*) is a moderately heavy tropical hardwood native to West Africa. It is a high-value tropical hardwood whose technological profile combines a fine, smooth, and lustrous texture with excellent natural durability and solid structural performance. It is widely used as a primary decorative substitute for American black walnut in cabinetmaking and is also applied for frames, parquet flooring, panelling, joinery, and building construction. It was also investigated as a raw material for producing three-layer plywood from veneers [60–63]. Mansonia has a diffuse-porous structure, weakly defined growth rings, and a distinctly coloured heartwood ranging

from yellowish-brown to dark greyish-brown. Its anatomical features include medium-length fibres, lack of tyloses in metaxylem vessels, calcium oxalate crystals in the rays, and parenchyma surrounding the vessels [61,62,64]. Its density typically ranges from 566 to 593 kg/m^3, with an MOE of approximately 9.3–14.7 GPa and an MOR of 114–177 MPa [46,62,65]. Mansonia shows relatively low shrinkage, with radial and tangential values of approximately 3.96% and 5.20%, respectively, and volumetric shrinkage of about 9.16%. The fibre saturation point is approximately 28%. The wood generally dries without major defects and has good dimensional stability. It also shows high natural resistance to fungal decay due to its heartwood extractives, although its low permeability makes impregnation difficult [62,66]. The species is suitable for veneer production, while the attractive wood grain pattern favours its use in furniture and other interior elements, such as floors and parquet. It also works well as elements of musical instruments [67].

Paulownia (*Paulownia* spp.) is a genus of fast-growing hardwood trees native to East Asia and widely cultivated in plantations, with potential applications in furniture, plywood, packaging, and engineered wood products. It is also considered for lightweight wood-based hybrid structures and for single-layer and three-layer paulownia solid wood panels, which can be used as lightweight core materials for furniture, packaging, and non-load-bearing applications [5,68–70]. Its wood has a ring-porous or semi-ring-porous structure, with large earlywood vessels, smaller latewood vessels, and multiseriate rays [67,71–73]. Paulownia is exceptionally lightweight, with oven-dry density typically ranging from 210 to 297 kg/m^3, categorising it as a low-density hardwood similar to balsa [67,71,74]. Its mechanical strength is relatively low, with an MOR of approximately 40–57 MPa and an MOE of 2.4–5.0 GPa [67,71,74–77]. The wood is characterised by low shrinkage and good dimensional stability, with volumetric shrinkage of approximately 8%. It dries rapidly and easily, with a low risk of cracking, warping, or other drying defects. Its low density and dimensional stability make it suitable for lightweight panels, furniture, packaging, and other non-load-bearing applications [74,78].

The industrial applications of the investigated wood species, which are commonly used in the production of flooring, furniture, joinery, veneers, and wood-based composites, highlight the importance of dimensional stability under varying environmental conditions [14,27,48,63]. Changes in relative humidity may induce moisture-related swelling of wood, affecting dimensional accuracy, surface flatness, component fit, and joint integrity. When swelling is restrained by adjacent elements, mechanical connections, or adhesive bonds, the resulting swelling pressure may generate internal stresses that can potentially lead to deformation or damage. Importantly, free swelling alone is insufficient to predict swelling pressure, as the latter also depends on the wood mechanical properties, anatomical direction, moisture conditions, and time-dependent stress relaxation [1,5,79]. Therefore, direct measurements of swelling pressure in the investigated wood species are essential for a more comprehensive assessment of their moisture-related behaviour and suitability for dimensionally constrained applications. Such measurements may also provide valuable information for improving joint and assembly design, determining appropriate dimensional allowances, and developing more reliable models of moisture-induced stresses in wood products.

Although information about the dimensional stability of tropical hardwoods is available in scientific literature, most investigations focus on free swelling, shrinkage, moisture sorption or the effects of wood modification on wood physical properties [13,21,24,35,37,47,48,63]. Swelling pressure has so far been studied mainly in temperate species and in a few, usually isolated, comparisons. Al-Musawi et al. [5] compared paulownia with Norway spruce, i.e., a plantation hardwood with a softwood, while Zauer et al. [8] examined the effect of anatomical direction in beech and spruce. These studies show that swelling pressure depends on species and direction, but they do not show

whether the differences hold among commercially important tropical hardwoods that are similar in density, nor whether density and stiffness can then serve as predictors. To our knowledge, no study has measured the magnitude, radial/tangential anisotropy, and time course of swelling pressure in several tropical hardwoods under a single protocol (identical specimen geometry, oven-dry start, immersion in water, full restraint), along with density and compressive MOE measured on the same material.

Therefore, this study compares six tropical hardwoods widely used for flooring, decking and joinery (sapele, khaya, framiré, tauari, abura, mansonia) with plantation paulownia as a low-density reference. We specifically test (i) whether density and direction-specific MOE explain differences in maximum swelling pressure, (ii) whether species of nearly identical density (568–578 kg/m^3) nevertheless differ in swelling pressure, and (iii) whether the R/T anisotropy and the rate of pressure development are species-specific.

2. Materials and Methods

2.1. Materials

The research material was straight-grained wood of seven tropical wood species, including sapele (*Entadrophragma cylindricum* Sprague), African mahogany (*Khaya ivorensis* A. Chev.), framiré (*Terminalia ivorensis* A. Chev.), tauari (*Couratari tauari*), abura (*Hallea ciliata* P.), mansonia (*Mansonia altissima* A. Chev.), and paulownia (*Paulownia tomentonsa* (Thunb.) Steud.). Wood from the first six species was purchased as decking boards from commercial timber merchants in the Wielkopolska region of Poland. Paulownia was obtained from a plantation in the Wielkopolska region, Poland.

Prior to the experiment, the wood was stored under stable temperature and humidity conditions (22 ± 3 °C, 60% relative air humidity). Heartwood parts of the selected species were cut into small specimens with dimensions 30 mm × 30 mm × 10 mm (in the tangential, radial, and longitudinal anatomical directions, respectively). All specimens were free from visual structural defects, grain deviations, knots, reaction wood, mould and soft rot, with annual rings oriented parallel to the tangential face of specimens. For each species, 24 specimens were prepared, forming 12 pairs of neighbouring specimens cut from the same board. Six pairs (12 specimens) were used for swelling pressure measurements in the tangential direction and six pairs (12 specimens) in the radial direction. An additional 30 mm × 30 mm × 30 mm specimens, twin to the pairs, were prepared for the modulus of elasticity mesurements (Section 2.2.3).

2.2. Methods

2.2.1. Density and Moisture Content Measurements

The density of the tropical wood specimens was determined by a stereometric method in accordance with ISO 13061-2 [80]. Prior to the measurements, the wooden blocks were conditioned for two weeks at 23 ± 2 °C and 60 ± 3% relative humidity. Subsequently, the dimensions of the samples were measured using a digital calliper with an accuracy of ±0.01 mm, and their mass was determined using an analytical balance (Sartorius GmbH, Göttingen, Germany) with an accuracy of 0.001 g. Prior to the experiment, all specimens had been stored for an extended period under normal laboratory conditions (see Section 2.1). Immediately before the measurements, they were additionally conditioned for two weeks at 23 ± 2 °C and 60 ± 3% relative humidity. Because of the long previous storage and the two-week final conditioning, the specimens can be assumed to have reached moisture content close to equilibrium with the surrounding air. This was not assumed to be identical for all species, so the moisture content of the specimens was determined by the oven-drying method. The mean values ranged from

11.1% (sapele) to 12.5% (paulownia). Density was calculated from the mass and volume of the specimens at this moisture content.

For swelling measurements, all wood samples were oven-dried at 103 ± 2 °C until a constant weight was reached. Their mass and dimensions were then determined.

2.2.2. Swelling Pressure

Wood total swelling pressure was measured on oven-dried blocks in the tangential and radial directions using a prototype device designed for this purpose (Figure 1) [81]. The apparatus consisted of a stand (1 in Figure 1) equipped with two frames (2 and 3 in Figure 1) that could move relative to each other. The position of the lower frame (3 in Figure 1) was adjusted using a screw (5 in Figure 1). The upper frame (2 in Figure 1) was connected to a dynamometer (bow type) (4 in Figure 1) to measure the swelling force and to a crossbar that supported a dial micrometre (6 in Figure 1). A container (7 in Figure 1) holding a specimen (8 in Figure 1) was placed on the lower shelf of the upper frame. The weight of the upper frame was balanced by counterweights (9 in Figure 1) to prevent tensile forces from acting on the unloaded dynamometer. The equipment enabled measurement of the total force required to counteract the specimen's linear swelling during wetting.

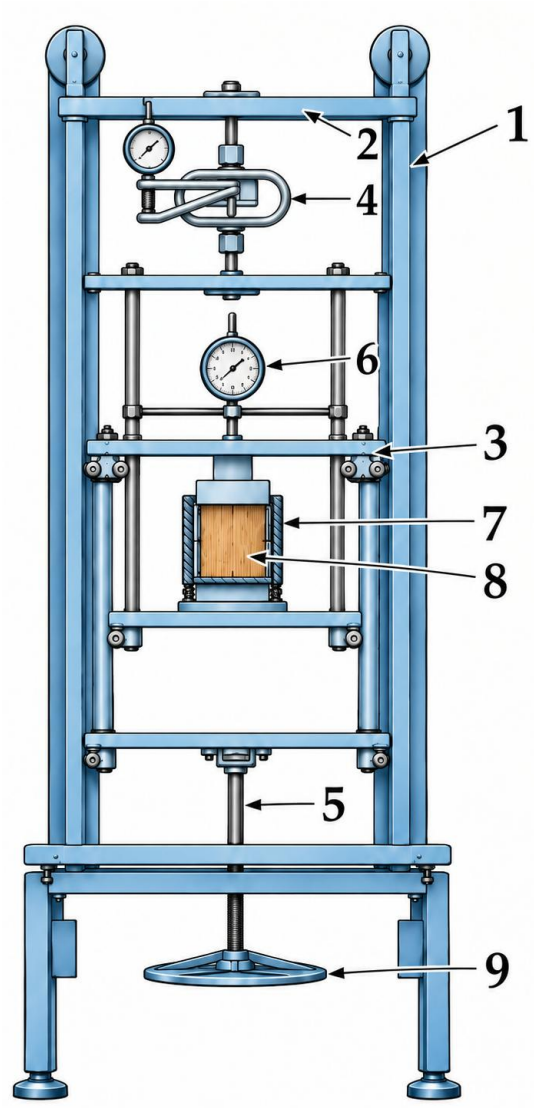


Figure 1. Diagram of a prototype apparatus used for the measurement of wood swelling pressure; 1—a stand; 2 and 3—slidable frames; 4—dynamometer; 5—adjusting screw; 6—dial micrometre; 7—container filled with water; 8—sample; 9—weights [82].

Before testing, each specimen was subjected to an initial preload to eliminate contact deformations. The measurement procedure was initiated by filling the container with water, causing the specimen to swell. As swelling progressed, the piston resting on the specimen was displaced upward and protruded from the container, causing the upper frame to descend. This displacement, corresponding to the specimen's swelling, was recorded using a dial micrometre. Once an initial swelling displacement of approximately 0.002 mm was detected, the lower frame was moved downwards using the adjusting screw. This adjustment compensated for swelling by applying compression, returning the dial micrometre needle to its initial position. The force required to counteract swelling at each measurement stage was recorded using the dynamometer. The bow dynamometer readings were initially taken after 30 s, then every minute (for 10 min), then every 5 min (for an hour) and finally every 15 min until the maximum swelling pressure was reached, as indicated by stabilisation or a decrease in the measured force. Swelling pressure was calculated based on Equation (1):

$$SP = \frac{F}{A} \quad (1)$$

where SP is the total swelling pressure (MPa), F is the value of swelling force measured (N), and A is the cross-sectional area of the sample in a completely dry state before the measurement. Two specimens were measured together as a pair, and each pair was treated as a single sample. In this way, six samples (pairs) per species were obtained in each of the tangential and radial directions, i.e., 12 samples per species in total.

2.2.3. Modulus of Elasticity

Since wood swelling pressure depends on the elastic modulus (*MOE*) in the direction of restrained swelling, increasing with an increase in MOE [4,83], the modulus of elasticity for the selected wood species was measured to help clarify the differences between them. *MOE* was measured during compression tests in the tangential and radial directions using a numerically controlled Zwick Z050TH (Zwick/Roell, Ulm, Germany) universal testing machine. Wood specimens with the dimensions 30 mm × 30 mm × 30 mm were used in the experiment. Measurements were taken with a loading speed of 1 mm/min. *MOE* was determined from the relationship between compressive stress and strain within the approximately linear-elastic region of the stress–strain curve [84,85]. For each species, 12 specimens (30 mm × 30 mm × 30 mm) were prepared as twins of the specimen pairs used for the swelling pressure tests, i.e., cut from the same boards in their immediate neighbourhood. *MOE* was reported as the mean value of 12 specimens per species in each direction.

2.2.4. Statistics

The experimental data were statistically analysed using STATISTICA 13.3 software (TIBCO Software Inc., Palo Alto, CA, USA). One-way analysis of variance (ANOVA) was performed to identify statistically significant differences between mean values. Differences between radial and tangential swelling pressure within each species were tested with Welch's *t*-test, with Holm correction for seven comparisons.

3. Results and Discussion

Mean density at 12% moisture content ranged from 357 kg/m³ (paulownia) to 707 kg/m³ (sapele) (Table 1). Abura, mansonia, khaya and framiré formed a group whose means differed by only 10 kg/m³ (568–578 kg/m³), so density alone is unlikely to explain differences in swelling pressure among them. Variability was low for most species (CV ≤ 1.64%; khaya 2.94%) but high for framiré (CV = 10.47%; range 515–648 kg/m³).

Table 1. Wood density of the selected wood species (n = 12 pairs per species).

Material	ϱmin	ϱmean	ϱmax	(±SD)	MC
	[kg·m⁻³]				[%]
Abura	562	**569** ^{b}	577	5.27	12.2
Mansonia	564	**572** ^{b}	583	7.35	11.4
Paulownia	352	**357** ^{a}	362	3.41	12.5
Tauari	608	**620** ^{c}	636	10.14	12.0
Khaya	546	**568** ^{b}	602	16.70	11.5
Framiré	515	**578** ^{b,c}	648	60.50	11.8
Sapele	693	**707** ^{d}	715	7.39	11.1

Note: Means within the same column that share identical superscript letters are not significantly different ($\alpha = 0.05$).

The density of abura, tauari, khaya and sapele fell within the ranges given in the Holzatlas [86], although the means of khaya, framiré and sapele were 11.4%, 15.6% and 8.8% higher than the Holzatlas means, and the maximum for framiré (648 kg/m³) exceeded the upper limit of its range (600 kg/m³). The mean for mansonia (572 kg/m³) was slightly below the lower limit of its range (580 kg/m³), and the density of paulownia (352–362 kg/m³) exceeded the range reported by Kozakiewicz (190–320 kg/m³) [67]. The density of paulownia in this study (352–362 kg/m³) is high for this genus, but it is within the wide range reported in the literature, where values vary considerably between species, hybrids, plantations and tree age, from about 210 to 350 kg/m³ and, according to some authors, up to about 400 kg/m³ [87–90]. Differences in density between species were tested with Welch's one-way ANOVA, because variances were heterogeneous (Bartlett's test, $p < 0.001$). Density differed significantly among species ($p < 0.001$). Paulownia (357 kg/m³) and sapele (707 kg/m³) differed significantly from all other species, and tauari (620 kg/m³) from abura, mansonia and khaya. Abura, mansonia, khaya and framiré (568–578 kg/m³) formed a homogeneous group, and the high variability of framiré (CV = 10.47%) prevented it from being distinguished from tauari.

Compressive *MOE* was highest in the longitudinal direction (4263–12 086 N/mm²), lower in the radial direction (475–2251 N/mm²) and lowest in the tangential direction (362–1545 N/mm²) in all species (Table 2), with mean ratios of 6.3 (L/R), 9.2 (L/T) and 1.6 (R/T).

Table 2. Compressive modulus of elasticity (mean ± SD, N/mm²; n = 12; coefficient of variation in brackets) in the longitudinal (L), radial (R) and tangential (T) directions.

Species	L	R	T
Paulownia	4263 ± 142 (3.3%)	475 ± 46 (9.8)	362 ± 5 (1.5)
Abura	5900 ± 901 (15.3%)	1497 ± 49 (3.3)	562 ± 28 (5.0)
Tauari	6701 ± 801 (11.9%)	961 ± 82 (8.6)	868 ± 53 (6.1)
Framiré	6754 ± 627 (9.3%)	1120 ± 38 (3.4)	661 ± 31 (4.7)
Mansonia	8117 ± 992 (12.2%)	1077 ± 83 (7.7)	880 ± 44 (5.0)
Khaya	9774 ± 1601 (16.4%)	1933 ± 56 (2.9)	1309 ± 48 (3.7)
Sapele	12,086 ± 1546 (12.8%)	2251 ± 114 (5.1)	1545 ± 178 (11.5)

Sapele had the highest *MOE* in every direction, and paulownia had the lowest. Variability was greatest along the grain (CV 3.3–16.4%) and smaller in the radial and

tangential directions (CV up to 9.8% and 11.5%). ANOVA showed significant differences among species in each direction (all $p < 0.001$). *MOE* was also positively related to mean density (r = 0.75–0.77, $p = 0.04$–0.055, n = 7 species), but species of similar density differed markedly in stiffness: khaya and abura (about 569 kg/m³) had longitudinal *MOE* values of 9774 and 5900 N/mm², so density alone does not explain stiffness.

MOE increased with density in all three directions (Figure 2): longitudinal $MOE_L = 19.1\varrho - 3178$ ($R^2 = 0.60$, $p = 0.041$), tangential $MOE_T = 2.98\varrho - 806$ ($R^2 = 0.57$, $p = 0.051$) and radial $MOE_R = 4.29\varrho - 1106$ ($R^2 = 0.56$, $p = 0.055$; n = 7 species). The three directions were strongly correlated with each other across species (r = 0.86–0.98), and the relationships were driven largely by the lightest and the densest species: after excluding sapele, R^2 fell to 0.39, 0.35 and 0.34, and without both paulownia and sapele, to 0.11 (L), 0.00 (T) and 0.37 (R), none of which was significant. The remaining five species had similar densities (568–620 kg/m³), but their *MOE* differed markedly, from 5900 to 9774 N/mm² in the longitudinal direction. Khaya was above the regression lines in all directions (by about 2100, 420 and 600 N/mm² in L, T and R), whereas tauari was below them (by about 1960, 170, and 600 N/mm²). This indicates that density explains the difference between the lightest and the heaviest species but not the differences among species of similar density, which are likely related to other features of wood structure [91–94].

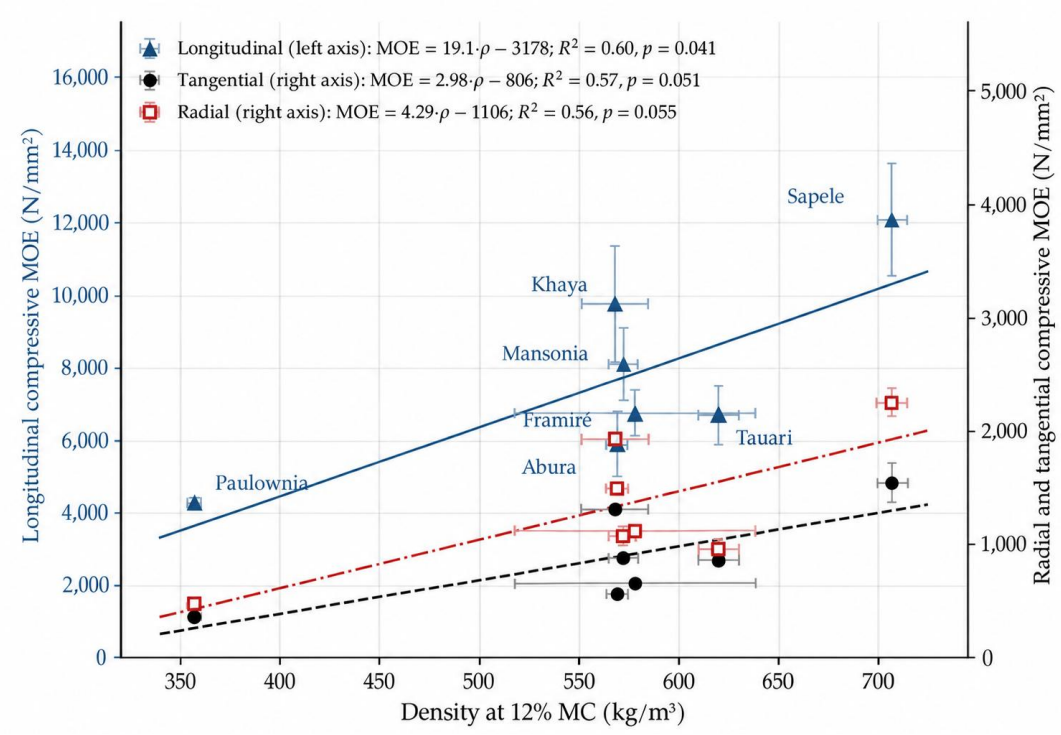


Figure 2. Relationship between density and longitudinal compressive MOE of the investigated wood species.

The maximum swelling pressure, determined as the mean of the maximum values reached by the individual replicates, ranged from 1.81 to 7.00 MPa in the tangential direction and from 1.17 to 8.85 MPa in the radial direction (Table 3). In both directions, it was lowest in paulownia and highest in sapele. The relationship between radial and tangential swelling pressures differed among species, as shown in Figure 3.

Table 3. Maximum swelling pressure in the tangential and radial directions (mean ± SD; coefficient of variation in brackets; n = 6 replicates per species).

Species	Tangential, MPa	Radial, MPa

Paulownia	1.81 ± 0.06 (3.5%)	1.17 ± 0.06 (5.3%)
Abura	3.03 ± 0.49 (16.3%)	2.27 ± 0.13 (5.5%)
Tauari	6.55 ± 0.10 (1.6%)	7.40 ± 0.87 (11.8%)
Framiré	4.12 ± 0.73 (17.8%)	5.89 ± 0.86 (14.7%)
Mansonia	2.90 ± 0.19 (6.6%)	2.76 ± 0.35 (12.6%)
Khaya	4.95 ± 0.60 (12.2%)	6.86 ± 0.70 (10.3%)
Sapele	7.00 ± 0.37 (5.3%)	8.85 ± 0.31 (3.5%)

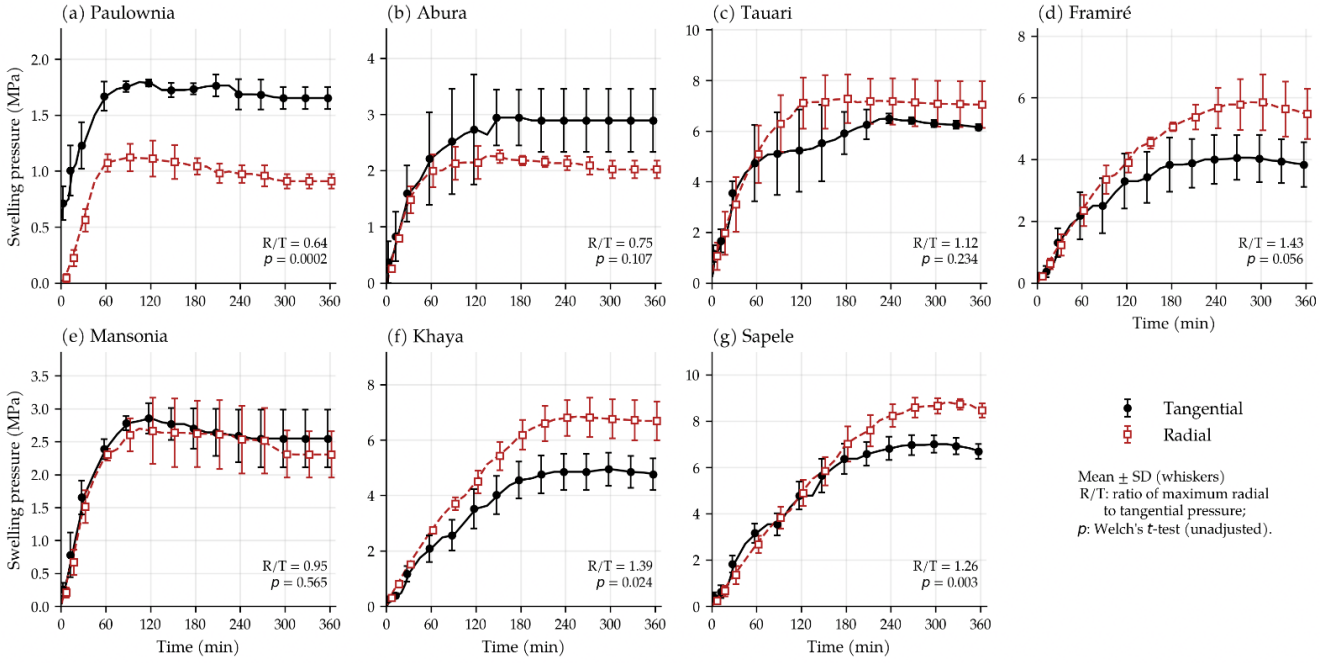


Figure 3. Changes in swelling pressure over time in the tangential (circles, solid line) and radial (squares, dashed line) directions for (**a**) paulownia, (**b**) abura, (**c**) tauari, (**d**) framiré, (**e**) mansonia, (**f**) khaya and (**g**) sapele. Points are mean values with ±SD (whiskers), n = 6. R/T is the ratio of the maximum radial to the maximum tangential swelling pressure, and *p* is the result of Welch's *t*-test for the difference between the two directions (not adjusted for multiple comparisons). Note the different vertical scales.

In sapele, khaya and framiré, the maximum radial pressure was significantly higher than the tangential one (R/T = 1.26, 1.39 and 1.43; $p < 0.0001$, $p = 0.0005$ and $p = 0.003$, respectively; all significant after Holm correction). In tauari, the radial pressure was slightly higher (R/T = 1.13), but the difference was not significant ($p = 0.062$; 0.12 after correction), and in mansonia the two directions did not differ (R/T = 0.95, $p = 0.42$). Abura and paulownia were the only species in which the tangential pressure was significantly higher (R/T = 0.75, $p = 0.011$, 0.034 after correction; R/T = 0.65, $p < 0.0001$). Since density is the same for both directions within a species, it cannot explain these differences. The ratio of radial to tangential *MOE* was above 1 in all species (1.11–2.66), but it did not predict the ratio of swelling pressures ($r = -0.23$, $p = 0.61$, n = 7); for instance, abura had the largest *MOE* ratio (2.66) but a lower radial than tangential pressure (R/T = 0.75). A simple index of the pressure developed relative to stiffness (*SP*/*MOE*) was higher in the tangential than in the radial direction in six of seven species (for example, 5.0 vs. 2.5‰ in Paulownia and 5.4 vs. 1.5‰ in abura), which is consistent with the greater tangential than radial swelling typical of wood [3,5,8,95,96]. Tauari was the exception, with practically equal values in the two directions (7.6 and 7.7%). The *SP*/*MOE* index should be interpreted with caution. Free-swelling strains were not measured in this study, and *MOE* was determined in the conditioned state, not at the moisture contents prevailing during swelling. The index

therefore cannot separate the contribution of swelling strain from that of stiffness. A possible explanation is that higher radial stiffness partly compensates for lower radial swelling in the denser, stiffer species (sapele, khaya, framiré), but not in the lighter ones (paulownia, abura). This remains a hypothesis, to be tested by measuring swelling coefficients and *MOE* at defined moisture contents on the same specimens.

The curves also differed in time. In most species, the radial pressure reached its maximum earlier than the tangential one (tauari after about 180 vs. 240 min, Khaya 255 vs. 300, Abura 135 vs. 150, Paulownia 90 vs. 105 and mansonia 105 vs. 120 min), whereas in Sapele and Framiré it came later in the radial direction (315 vs. 300 and 285 vs. 270 min). In the species with the highest radial pressures, the radial curve rose more slowly at the start: after 60 min, Sapele had reached 30% of its maximum radial pressure, compared with 45% in the tangential direction. After the maximum, the radial pressure decreased more strongly in paulownia, abura and mansonia (19%, 11% and 15% at 360 min) than the tangential pressure (8%, 2% and 11%).

The curves of tangential swelling pressure (Figure 4) had a similar general shape in all species: a rapid increase during the first hour, a slower increase, a plateau and a slight decrease towards the end of the test. However, the species differed clearly in how quickly the pressure developed. Paulownia, mansonia and abura built up pressure fastest relative to their maxima: after 60 min, they had reached 93%, 84% and 75% of their maxima, and reached their maxima after about 105, 120 and 150 min, respectively. Because these species also reached the lowest maxima (1.8–2.9 MPa), a quick but small response characterised the group. Sapele and khaya were at the opposite extremes, reaching only 45% and 42% of their maxima after 60 min, and about 90% after 180 min, peaking at about 300 min. Framiré behaved similarly but somewhat faster (reaching 54% of its maximum after 60 min, peaking at about 270 min).

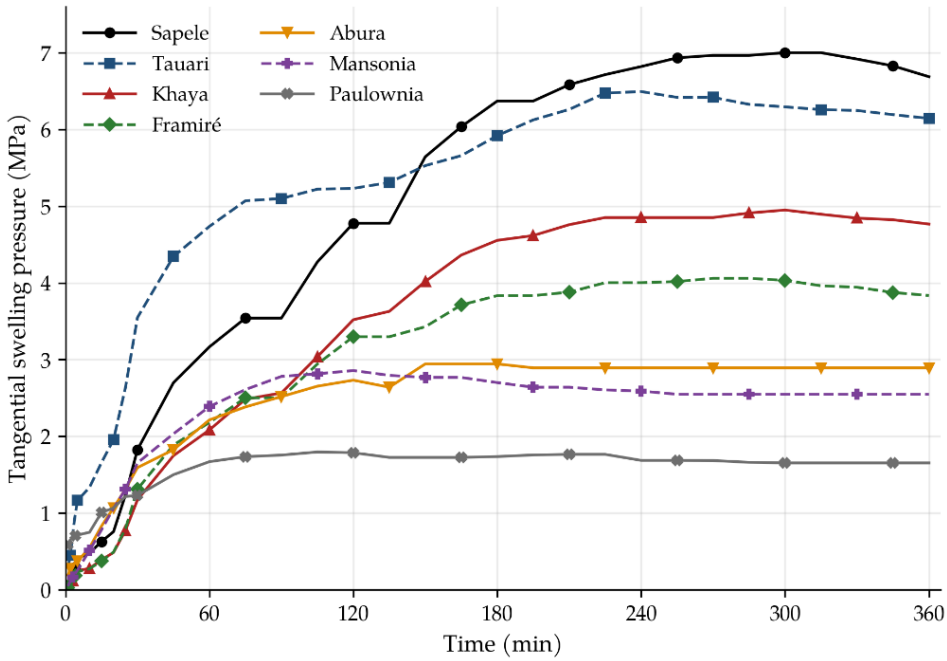


Figure 4. Changes in tangential swelling pressure over time for the investigated species.

Tauari did not fit this pattern. Its pressure rose very rapidly at the beginning (3.6 MPa, or 55% of the maximum, after 30 min, compared with 1.8 MPa for Sapele and 1.2 MPa for Khaya), then increased only slowly until a maximum at about 240 min. As a result, tauari had the highest pressure among all species for the first 120 min, and sapele overtook it only after about 150 min, finishing with the highest maximum (7.00 vs. 6.55

MPa). Thus, the species with the highest final pressures were not the ones that developed it fastest. Differences in the rate of pressure development may be related to differences in moisture uptake, which depends on the permeability and anatomical structure of the wood [5,19,97,98], but the present data do not allow this to be confirmed.

After reaching their maximum, all curves decreased slightly, by about 2% (abura) to 11% (mansonia) at 360 min. This curve, with a maximum followed by a gradual decrease, is typical of the development of swelling pressure in restrained wood and has been reported previously [3,5,12]. The decrease is commonly attributed to viscoelastic relaxation of the restrained wood [3,99,100]. The variability between replicates also differed among species: during the plateau, the coefficient of variation between the six replicates was about 1.6% for tauari and 3.5–6.6% for sapele, paulownia and mansonia, but 12.2–17.8% for khaya, framiré, and abura. The mean curves of the latter species should therefore be interpreted with more caution.

Radial swelling pressure increased with time in all species and then levelled off or declined slightly (Figure 5). The maximum values differed significantly among species ($p < 0.001$): sapele (8.85 MPa), tauari (7.40 MPa) and khaya (6.86 MPa) reached the highest pressures, framiré (5.89 MPa) was intermediate, and mansonia (2.76 MPa), abura (2.27 MPa) and paulownia (1.17 MPa) the lowest. Sapele, tauari, and khaya differed significantly from abura, mansonia, and paulownia ($p < 0.05$), whereas framiré differed only from paulownia, and abura also differed from paulownia. The species also differed in the rate of pressure development.

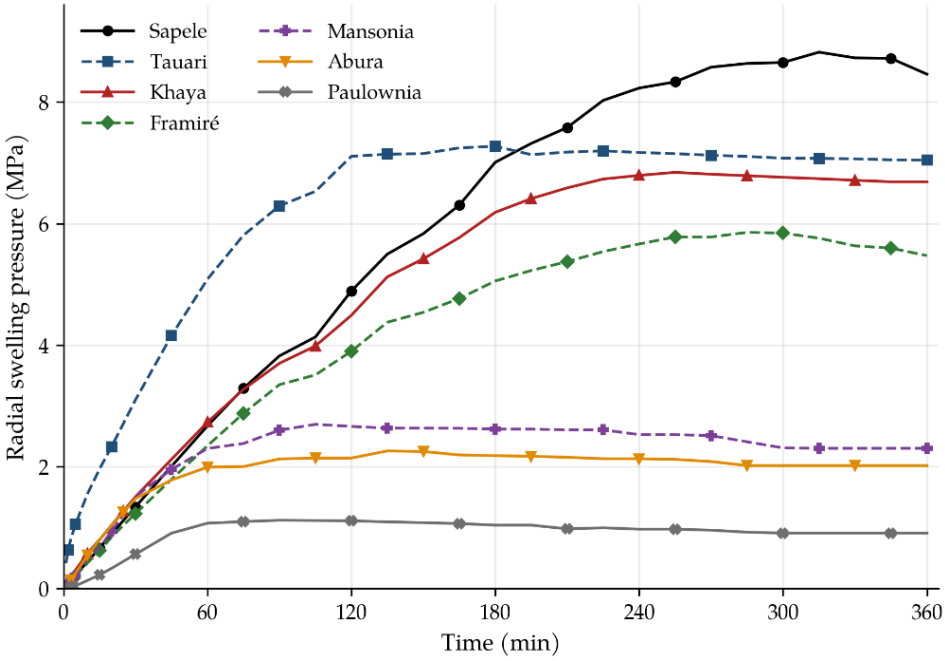


Figure 5. Changes in radial swelling pressure over time for the investigated species.

Paulownia, mansonia, and abura reached 96%, 85%, and 88% of their maximum after 60 min and peaked at about 90–135 min. Tauari rose fastest among the high-pressure species (3.1 MPa after 30 min and 98% of its maximum after 120 min), whereas khaya, framiré and Sapele reached only 30–40% of their maxima after 60 min and peaked after about 255–315 min. Sapele overtook tauari after about 195 min and finished with the highest pressure. After the maximum, the pressure decreased slightly across all species, by about 2–4% in khaya, tauari, and sapele, but by 11–19% in abura, mansonia, and paulownia, which had the lowest pressures. Maximum radial swelling pressure exceeded

the tangential one in khaya, framiré, sapele and tauari (ratios of 1.4, 1.4, 1.3 and 1.1) but was lower in abura, mansonia and paulownia (0.75, 0.95 and 0.65).

Maximum swelling pressure increased with density in both directions (Figure 6). In the tangential direction, the linear model was $SP = 0.0151\rho - 4.25$ ($R^2 = 0.68$, $p = 0.023$, n = 7 species), and in the radial direction, $SP = 0.0220\rho - 7.45$ ($R^2 = 0.62$, $p = 0.036$). The slope was steeper in the radial direction, but the 95% confidence intervals of the two slopes overlapped widely (0.0151 ± 0.0120 and 0.0220 ± 0.0198), and the maxima in the two directions were strongly correlated across species (r = 0.96, $p < 0.001$).

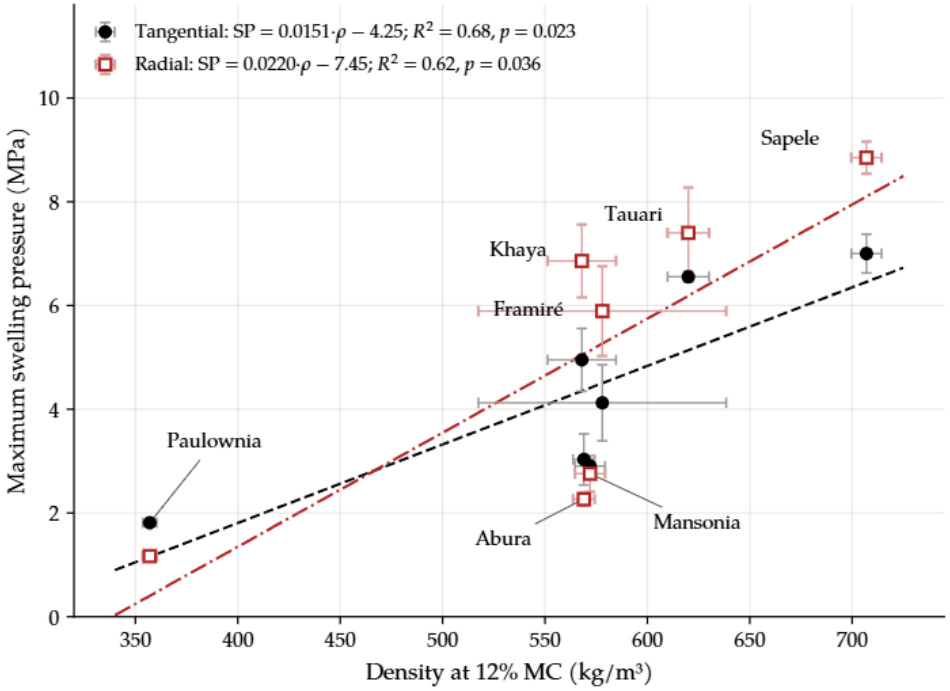


Figure 6. Relationship between density at 12% moisture content and maximum tangential (circles) and radial (squares) swelling pressure of the investigated species. Points are species means (± SD); lines show the linear regressions.

The lightest species, paulownia (357 kg/m³), had the lowest pressure in both directions (1.81 and 1.17 MPa), and the densest, sapele (707 kg/m³), had the highest (7.00 and 8.85 MPa). The relationship was largely determined by these two species: when sapele was excluded, R^2 fell to 0.53 ($p = 0.10$) in the tangential and 0.46 ($p = 0.14$) in the radial direction, and without both species, to 0.66 ($p = 0.09$) and 0.33 ($p = 0.31$). Density did not distinguish species, with nearly identical density: khaya, framiré, abura, and mansonia (568–578 kg/m³) had maximum tangential pressures ranging from 2.90 to 4.95 MPa and radial pressures from 2.27 to 6.86 MPa. Tauari (620 kg/m³) developed higher pressures than predicted (about 1.4 MPa above the tangential and 1.2 MPa above the radial line), whereas abura and mansonia lay well below the lines, particularly in the radial direction (by about 2.4–2.8 MPa).

Maximum swelling pressure increased with compressive *MOE* measured in the same direction (Figure 7). In the tangential direction the linear model was SP = 0.0036·MOE_T + 1.14 ($R^2 = 0.61$, $p = 0.039$, n = 7 species), whereas in the radial direction the relationship was weaker and not significant ($SP = 0.0032 \cdot MOE_R + 0.83$; $R^2 = 0.42$, $p = 0.114$). The slopes in the two directions were similar (0.0036 ± 0.0034 and 0.0032 ± 0.0042 MPa per N/mm², 95% CI), so the difference between the directions lies mainly in the scatter of the points.

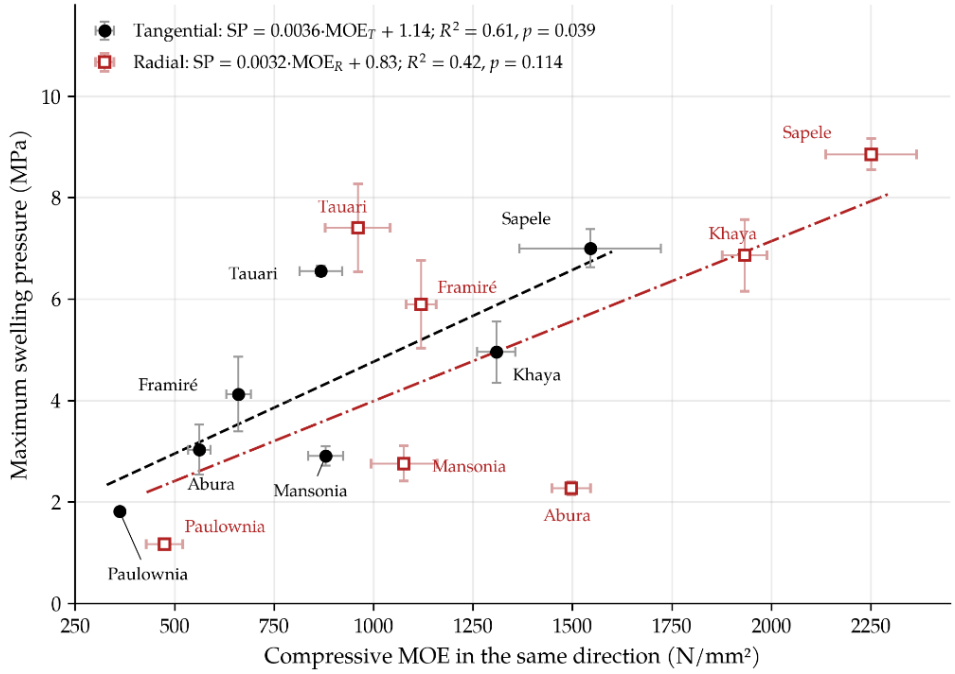


Figure 7. Relationship between compressive modulus of elasticity (MOE) and maximum swelling pressure in the tangential (circles) and radial (squares) directions. Points are species means (± SD); lines show the linear regressions.

The observed increase in swelling pressure with wood density is consistent with the findings of Zauer et al. [8], who attributed the higher swelling pressure in beech than in spruce to a higher proportion of cell-wall material and higher resistance to compression. However, the considerable differences between species of similar density suggest that density alone cannot adequately describe the mechanisms governing swelling pressure. Kanno [101] demonstrated that swelling stress is related to both the transverse *MOE* and the swelling coefficient, indicating that mechanical stiffness should be considered together with moisture-induced deformation. The deviations observed for tauari, abura and mansonia may therefore reflect species-specific anatomical characteristics, including differences in vessel distribution, ray structure and cell-wall organisation, which are known to influence the mechanical properties of hardwoods [102]. Furthermore, the pressure developed under restrained swelling is influenced not only by elastic stiffness but also by moisture-dependent material behaviour and stress relaxation, particularly through viscoelastic and mechano-sorptive effects [5,12]. The similar regression slopes and overlapping confidence intervals obtained for the tangential and radial directions suggest that the sensitivity of swelling pressure to *MOE* may be comparable in both directions, despite differences in the strength of the correlations. Nevertheless, the limited number of analysed species and the influence of extreme values indicate that these relationships should be interpreted with caution and that incorporating swelling coefficients and anatomical characteristics may improve predictions of swelling pressure across different wood species.

Species with the lowest *MOE* (paulownia, abura) developed the lowest pressures and those with the highest (sapele, khaya) the highest, but the relationship was determined largely by paulownia and sapele: without sapele, R^2 fell to 0.39 in the tangential and 0.19 in the radial direction, and without both species to 0.16 and 0.00. The scatter around the lines was large. Tauari developed a much higher pressure than expected from its *MOE* (about 2.3 MPa above the tangential and 3.5 MPa above the radial line), abura had a much lower radial pressure than expected (about 3.3 MPa below the line), and mansonia lay

below both lines. Compared with density (Figure 5; $R^2 = 0.68$ tangential, 0.62 radial), *MOE* explained somewhat less of the variation in swelling pressure, especially in the radial direction.

These results agree with Kollmann [103], who reported that swelling pressure increases with wood density and with the transverse modulus of elasticity. In the present study, the maximum swelling pressure increased with density in both directions (Figure 5) and with *MOE* in the tangential direction (Figure 6), whereas the relationship with radial *MOE* was weaker and not significant. Because *MOE* generally increases with density [104–106], the two properties are partly interrelated, as shown by their positive correlation across the investigated species ($r = 0.75–0.77$, $p = 0.04–0.055$, $n = 7$). The relationship was not exact, however, because species of similar density (568–578 kg/m^3) differed markedly in MOE and swelling pressure.

The differences in swelling pressure observed among the investigated tropical hardwood species and paulownia may be partly attributed to their anatomical structure, which influences both moisture transport and mechanical behaviour. It has already been reported that vessel distribution and dimensions, pit connectivity, and ray content and structure affect water movement within wood tissue, while cell-wall thickness, wood density, and cellulose microfibril orientation in the cell wall contribute to the wood mechanical stiffness [102,107]. In particular, it has been shown that vessels may reduce wood tissue stiffness, while rays can provide some reinforcement in the radial direction, proving the significance of wood anatomical organisation to its mechanical behaviour [108]. Moreover, it is known that moisture penetration into the cell walls induces hygroscopic expansion, which generates internal stresses when dimensional changes are restrained [109]. Therefore, it can be concluded that wood swelling pressure results from the combined effects of moisture transport, cell-wall swelling capacity, transverse stiffness, and stress relaxation rather than by water uptake or unrestricted swelling alone [79]. All these structural and mechanical interactions may contribute to species-specific differences in swelling pressure; hence, further detailed studies including wood anatomical characterisation, moisture transport measurements, and mechanical testing are necessary to establish their effective contributions.

4. Conclusions

The results of this study clearly show that the swelling pressure of the investigated tropical species depends strongly on both the species and the anatomical direction. It was lowest in paulownia and highest in sapele in both the tangential and radial directions. In most of the denser, stiffer species (sapele, khaya, framiré), the radial pressure exceeded the tangential pressure, whereas it was significantly lower in the low-density paulownia. Species that developed the highest pressures were not always those that did so fastest, as shown by tauari, where the swelling pressure rose rapidly but reached a lower maximum than that of sapele.

Maximum swelling pressure increased with wood density in both anatomical directions. The relationship was significant in the tangential ($R^2 = 0.68$) and radial ($R^2 = 0.62$) directions. It was strongly influenced by wood density and particularly visible in the case of the lightest and densest species. However, wood species with similar densities, such as abura, mansonia, khaya, and framiré, exhibited considerably different swelling pressures, indicating that density alone is not sufficient to predict swelling pressure.

Swelling pressure was also positively related to the compressive modulus of elasticity. This relationship was statistically significant in the tangential direction ($R^2 = 0.61$), but not in the radial direction ($R^2 = 0.42$). This relationship was also driven largely by the lightest and the densest species, and species of similar density and stiffness differed markedly in swelling pressure. The results suggest that wood density and *MOE* are

therefore useful general indicators of the swelling pressure that can develop in restrained wood, but neither fully describes the differences between species nor allows prediction of the pressure values for individual species.

The relationship between radial and tangential swelling pressure was species-dependent. Radial pressure was significantly higher than tangential in sapele, khaya and framiré, and significantly lower in abura and paulownia, whereas no significant difference was found in tauari and mansonia (Welch's *t*-test, Holm-corrected). The ratio of radial to tangential *MOE* did not predict the corresponding ratio of swelling pressures, so within the limits of this study, swelling pressure anisotropy was not explained by differences in wood stiffness alone.

The rate of swelling pressure development also differed considerably between species. Paulownia, abura and mansonia reached relatively low maximum pressures within a short time, whereas sapele and khaya developed higher pressures more slowly. Tauari was an exception, showing both rapid initial pressure development and a high maximum pressure. These results indicate that the rate of pressure development and the maximum pressure are not directly related.

After reaching the maximum, swelling pressure decreased slightly in all investigated species. This behaviour is consistent with the viscoelastic relaxation of wood under restrained-swelling conditions. The differences in swelling pressure and its temporal development may also be related to the wood's anatomical structure and moisture transport properties. Further studies are needed to determine the contribution of these factors.

Overall, the findings indicate that swelling pressure is governed by a combination of species-specific characteristics, anatomical direction and time-dependent behaviour, with wood density and compressive stiffness providing only partial explanations of the observed variability. Nevertheless, because the study included only seven wood species and six replicates per species and anatomical direction, the results should be interpreted as general tendencies rather than definitive relationships. Further investigations involving larger sample sizes and detailed characterisation of wood anatomy and moisture transport properties are necessary to clarify the mechanisms responsible for differences in swelling pressure between species and anatomical directions and to improve its prediction under restrained moisture-induced swelling conditions.

Author Contributions: Conceptualization, P.M. and M.B.; methodology, P.M. and M.B.; validation, P.M. and M.B.; formal analysis, P.M.; investigation, M.S., F.C., P.M. and M.B.; data curation, P.M.; writing—original draft preparation, M.B. and P.M.; writing—review and editing, M.B., P.M., M.S., and F.C. visualization, P.M.; supervision, P.M. All authors have read and agreed to the published version of the manuscript.

Funding: This research received no external funding.

Institutional Review Board Statement: Not applicable.

Informed Consent Statement: Not applicable.

Data Availability Statement: The raw data supporting the conclusions of this article will be made available by the authors on request.

Acknowledgments: During the preparation of this manuscript, the authors used ChatGPT-6 to prepare the graphical abstract and a schematic of testing equipment based on a photograph of the original device (Figure 1). The authors have reviewed and edited the output and take full responsibility for the content of this publication.

Conflicts of Interest: The authors declare no conflicts of interest.

References

1. Engelund, E.T.; Thygesen, L.G.; Svensson, S.; Hill, C.A.S. A Critical Discussion of the Physics of Wood–Water Interactions. *Wood Sci. Technol.* **2013**, *47*, 141–161. https://doi.org/10.1007/s00226-012-0514-7.
2. Arzola-Villegas, X.; Lakes, R.; Plaza, N.Z.; Jakes, J.E. Wood Moisture-Induced Swelling at the Cellular Scale—Ab Intra. *Forests* **2019**, *10*, 996. https://doi.org/10.3390/f10110996.
3. Mazzanti, P.; Colmars, J.; Gril, J.; Hunt, D.; Uzielli, L. A Hygro-Mechanical Analysis of Poplar Wood along the Tangential Direction by Restrained Swelling Test. *Wood Sci. Technol.* **2014**, *48*, 673–687. https://doi.org/10.1007/s00226-014-0633-4.
4. Majka, J.; Roszyk, E. Swelling Restraint of Thermally Modified Ash Wood Perpendicular to the Grain. *Eur. J. Wood Wood Prod.* **2018**, *76*, 1129–1136. https://doi.org/10.1007/s00107-018-1321-0.
5. Al-musawi, H.; Emsenhuber, G.; Ungerer, B.; Baumann, G.; Feist, F.; Müller, U. Development of Swelling Pressure in Paulownia and Norway Spruce during Moisture Absorption. *Eur. J. Wood Wood Prod.* **2025**, *83*, 47. https://doi.org/10.1007/s00107-025-02204-4.
6. Perkitny, T.; Kingston, R.S.T. Review of the Sufficiency of Research on the Swelling Pressure of Wood. *Wood Sci. Technol.* **1972**, *6*, 215–229. https://doi.org/10.1007/BF00351579.
7. Rowell, R.M. One Way to Keep Wood from Going This Way and That. *Am. Rec.* **1995**, *36*, 12–16.
8. Zauer, M.; Porath, J.; Krüger, R.; Wagenführ, A. Investigations into the Swelling Pressure of Wood as a Function of the Anatomical Direction. *Phys. Open* **2025**, *22*, 100244. https://doi.org/10.1016/j.physo.2024.100244.
9. Arnold, D. *Building in Egypt: Pharaonic Stone Masonry*; Oxford University Press: New York, NY, USA, 1991.
10. El-Sehily, B.M. Fracture Mechanics in Ancient Egypt. *Procedia Struct. Integr.* **2016**, *2*, 2921–2928. https://doi.org/10.1016/j.prostr.2016.06.365.
11. Grönquist, P.; Schnider, T.; Thoma, A.; Gramazio, F.; Kohler, M.; Burgert, I.; Rüggeberg, M. Investigations on Densified Beech Wood for Application as a Swelling Dowel in Timber Joints. *Holzforschung* **2019**, *73*, 559–568. https://doi.org/10.1515/hf-2018-0106.
12. Stöcklein, J.; Grajcarek, G.; Konopka, D.; Kaliske, M. Hygro-Mechanical Long-Term Behaviour of Spruce, Pine and Lime Wood: Parameter Identification and Model Validation. *Wood Sci. Technol.* **2024**, *58*, 2007–2031. https://doi.org/10.1007/s00226-024-01577-8.
13. Korkut, S. Performance of Three Thermally Treated Tropical Wood Species Commonly Used in Turkey. *Ind. Crops Prod.* **2012**, *36*, 355–362. https://doi.org/10.1016/j.indcrop.2011.10.004.
14. Olenska, S.; Beer, P. Quality Evaluation of New Types of Core Layers Based on Different Thicknesses of Veneers for Flooring Materials. *Materials* **2024**, *17*, 5881. https://doi.org/10.3390/ma17235881.
15. Yakusu, E.K.; Monthe, F.S.; Bourland, N.; Hardy, O.J.; Louppe, D.; Lokanda, F.B.M.; Hubau, W.; Muhongya, J.-M.K.; Van den Bulcke, J.; Van Acker, J.; et al. Entandrophragma: Taxonomy and ecology of a genus of African tree species with economic importance. A review. *Biotechnol. Agron. Soc. Environ.* **2018**, *22*, 113–127.
16. Topaloğlu, E.; Ustaömer, D.; Ozturk, M. Investigation of Some Technological Properties of Three African Tropical Woods: Ayous, Iroko, Sapelli. *Kastamonu Univ. J. For. Fac.* **2025**, *25*, 220–232. https://doi.org/10.17475/kastorman.1787607.
17. Hızal, K.T.; Koçer, N. Macroscopic and Microscopic Diagnosis of Three Entandrophragma Species Traded in Türkiye. *BioResources* **2024**, *19*, 2575–2591. https://doi.org/10.15376/biores.19.2.2575-2591.
18. Yakusu, E.K.; Louppe, D.; Monthe, F.K.; Hardy, O.J.; Lokanda, F.B.M.; Hubau, W.; den Bulcke, J.V.; Acker, J.V.; Beeckman, H.; Bourland, N.; et al. Improved Management of Species of the African Entandrophragma Genus, Now Listed as Vulnerable. *Bois Forets Trop.* **2021**, *349*, 67–86. https://doi.org/10.19182/bft2021.349.a36791.
19. Manga Bengono, D.M.; Jean Gaston, T.; Joseph, Z.M.; Evariste, F.F.; Armand, F.L.; Fonyuy, B.G.; Achille Bernard, B. Sorption Behaviour of Three African Tropical Woods (Sapelli, Sipo, Kosipo) with Similar Anatomical Structures from Cameroon. *Int. Wood Prod. J.* **2022**, *13*, 194–202. https://doi.org/10.1080/20426445.2022.2073075.
20. Julien, N.C.; Stephane, N.N.; René, O.L.; Max, A.O.L. Viscoelastic Properties of Hardwood from the Congo Basin. *Int. Wood Prod. J.* **2025**, *16*, 301–309. https://doi.org/10.1177/20426445251387807.
21. Manga Bengono, D.M.; Biwole, A.B.; Zobo Mfomo, J.; Ouertani, S.; Tamba, J.G. Effect of Axial and Ray Parenchyma and Extractives on the Dimensional Stability of Three African Tropical Woods: Kosipo, Sapelli and Sipo. *Wood Mater. Sci. Eng.* **2026**, *21*, 525–540. https://doi.org/10.1080/17480272.2024.2437506.
22. Manga Bengono, D.M.; Tamba, J.G.; Zobo Mfomo, J.; Fopah-Lele, A.; Diboma, B.S.; Banyuy, F.G.; Biwolé, A.B. Influence of the Anatomical Structure on the Moisture Sorption and Thermodynamic Properties of the African Tropical Woods. *Heat Mass Transf.* **2023**, *59*, 113–130. https://doi.org/10.1007/s00231-022-03242-x.

23. Dadzie, P.K.; Amoah, M.; Frimpong-Mensah, K.; Oheneba-Kwarteng, F. Some Physical, Mechanical and Anatomical Characteristics of Stemwood and Branchwood of Two Hardwood Species Used for Structural Applications. *Mater. Struct.* **2016**, *49*, 4947–4958. https://doi.org/10.1617/s11527-016-0835-3.
24. de Carvalho, A.M.; da Silva, B.T.B.; Latorraca, J.V.D.F. Evaluation of machinability and characterization of the physical properties of African mahogany (Khaya ivorensis A. Chev.) wood. *Cerne* **2010**, *16*, 106–114.
25. Dadzie, P.K.; Amoah, M. Density, Some Anatomical Properties and Natural Durability of Stem and Branch Wood of Two Tropical Hardwood Species for Ground Applications. *Eur. J. Wood Wood Prod.* **2015**, *73*, 759–773. https://doi.org/10.1007/s00107-015-0925-x.
26. Oyebanji, J.A.; Oyedepo, S.O.; Oyebanji, O.T.; Araoyinbo, A.O.; Kilanko, O.; Dirisu, J.O.; Saleh, B. Experimental Investigation of Heating Values and Chemical Compositions of Selected Fuel Woods as Bio-Fuel Sources in Developing Countries. *Fuel* **2023**, *340*, 127600. https://doi.org/10.1016/j.fuel.2023.127600.
27. França, T.S.F.A.; França, F.J.N.; Arango, R.A.; Costa, A.; Ogunruku, M. Properties of African Mahogany Wood Commercially Available in the United States. *For. Prod. J.* **2024**, *73*, 339–349. https://doi.org/10.13073/FPJ-D-23-00055.
28. França, T.S.F.A.; Arantes, M.D.C.; Paes, J.B.; Vidaurre, G.B.; Oliveira, J.T.D.S.; Baraúna, E.E.P. Anatomical characteristics and wood physical-mechanical properties of two African mahogany species. *Cerne* **2015**, *21*, 633–640. https://doi.org/10.1590/01047760201521041877.
29. Oyedapo, O.A.; Ogunlowo, I.I.; Ojo, F.M.; Adenegan–Alakinde, T.A. Characterization of Three Khaya Species Used in Nigeria as a Medicinal Plants for Proper Identification Using Wood Anatomy. *Ife J. Sci.* **2025**, *27*, 921–932. https://doi.org/10.4314/ijs.v27i3.24.
30. Soranso, D.R.; Vidaurre, G.B.; Chagas, M.P.; Oliveira, J.T.D.S.; da Silva, J.G.M.; Latorraca, J.V.D.F. Radial Growth Dynamics of Khaya Ivorensis Trees from Experimental Plantation. *Rev. Árvore* **2018**, *42*, e420207. https://doi.org/10.1590/1806-90882018000200007.
31. Wepia Apungu, J.; Antwi, K.; Appiah-Kubi, E.; Kofi Bih, F.; Zakaria, J. Investigating Physical and Mechanical Properties of Mahogany Root Wood (Khaya Ivorensis) for Its Utilization. *Drv. Ind.* **2025**, *76*, 189–199. https://doi.org/10.5552/drvind.2025.0228.
32. Santos, L.H.D.O.; Alexandre, F.S.; de Mendoza, Z.M.D.S.H.; de Souza, É.C.; Borges, P.H.D.M.; Mariano, R.R.; Ruiz Diaz, L.M.G.; Nunes, C.A. Chemical and Physical Characteristics of African Mahogany Wood (Khaya Ivorensis A. Chev.). *Nativ. Pesqui. Agrár. Ambient.* **2020**, *8*, 361–366. https://doi.org/10.31413/nativa.v8i3.9526.
33. Jamala, G.Y.; Olubunmi, S.O.; Mada, D.A.; Abraham, P. Physical and Mechanical Properties of Selected Wood Species in Tropical Rainforest Ecosystem, Ondo State, Nigeria. *IOSR J. Agric. Vet. Sci.* **2013**, *5*, 29–33. https://doi.org/10.9790/2380-0532933.
34. Mohd-Jamil, A.; Khairul, M. Variations of Mechanical Properties in Plantation Timbers of Jelutong (Dyera Costulata) and Khaya (Khaya Ivorensis) Along the Radial and Vertical Positions. *J. Trop. For. Sci.* **2017**, *29*, 114–120.
35. Dadzie, P.K.; Amoah, M.; Ebanyenle, E.; Frimpong-Mensah, K. Characterization of Density and Selected Anatomical Features of Stemwood and Branchwood of *E. cylindricum*, *E. angolense* and *K. ivorensis* from Natural Forests in Ghana. *Eur. J. Wood Wood Prod.* **2018**, *76*, 655–667. https://doi.org/10.1007/s00107-017-1195-6.
36. Moomin, A.; Russell, W.R.; Knott, R.M.; Scobbie, L.; Mensah, K.B.; Adu-Gyamfi, P.K.T.; Duthie, S.J. Season, Storage and Extraction Method Impact on the Phytochemical Profile of Terminalia Ivorensis. *BMC Plant Biol.* **2023**, *23*, 162. https://doi.org/10.1186/s12870-023-04144-8.
37. Grubben, G.J.H. *Plant Resources of Tropical Africa (PROTA)*; Prota: Wageningen, The Netherlands, 2008.
38. Urbinati, C.V.; Azevedo, A.A.; da Silva, E.A.M.; Lisboa, P.L. Variação Estrutural Quantitativa No Lenho de Terminalia Ivorensis A. Chev., Combretaceae. *Acta Bot. Bras.* **2003**, *17*, 421–437. https://doi.org/10.1590/S0102-33062003000300009.
39. Antwi-Boasiako, C.; Apreko-Pilly, S. Tissue Dimensions and Proportions of the Stem and Branch Woods of *Aningeria robusta* (A. Chev) and *Terminalia ivorensis* (A. Chev). *Afr. J. Wood Sci. For.* **2016**, *4*, 254–273.
40. Okoh, E.T. Fibre, Physical and Mechanical Properties of Ghanaian Hardwoods. *J. Energy Nat. Resour.* **2014**, *3*, 25–30. https://doi.org/10.11648/j.jenr.20140303.11.
41. Amoah, M.; Appiah-Yeboahand, J.; Okai, R. Characterization of Physical and Mechanical Properties of Branch, Stem and Root Wood of Iroko and Emire Tropical Trees. *Res. J. Appl. Sci. Eng. Technol.* **2012**, *4*, 1755–1761.
42. Antwi-Boasiako, C.; Atta-Obeng, E. Vessel-Fibre Ratio, Specific Gravity and Durability of Four Ghanaian Hardwoods. *J. Sci. Technol.* **2009**, *29*, 50046. https://doi.org/10.4314/just.v29i3.50046.
43. Mahari, A.; Eshete, G.; Kolleh, D.M.; Watson, A.T.; Watson, R. Evaluation of Naturally Grown Termite Resistant Tropical Wood Species. *Asian J. Environ. Ecol.* **2024**, *23*, 1–7. https://doi.org/10.9734/AJEE/2024/v23i2523.

44. Mohammed, A.I.; Ejeh, S.P.; Amartey, Y.D.; Ocholi, A. Determined Uncertainty Models of Reference Material Properties and the En 338 Strength Class of Nigerian Grown Terminalia Ivorensis (Black Afara) Timber. *Niger. J. Technol.* **2019**, *38*, 302–313. https://doi.org/10.4314/njt.v38i2.5.
45. Okai, R.; Frimpong-Mensah, K.; Yeboah, D. Characterization of Strength Properties of Branchwood and Stemwood of Some Tropical Hardwood Species. *Wood Sci. Technol.* **2004**, *38*, 163–171. https://doi.org/10.1007/s00226-004-0232-x.
46. Adetayo, O.A.; Dahunsi, B.I.O. Fire Resistance Properties of Some Selected Tropical Timber Species from South-Western Nigeria after Fire Exposure. *Sel. Sci. Pap. J. Civ. Eng.* **2020**, *14*, 61–72. https://doi.org/10.1515/sspjce-2019-0018.
47. Andrade, F.W.C.; Moutinho, V.C.P.; Severo, E.T.D.; Ferreira, J.S.d.S.; Ballarin, A.W. Impact of Thermal Modification on Swelling and Mechanical Behavior of *Couratari* spp. *BioResources* **2023**, *18*, 5242–5252.
48. Laskowska, A.; Marchwicka, M.; Trzaska, A.; Boruszewski, P. Surface and Physical Features of Thermo-Mechanically Modified Iroko and Tauari Wood for Flooring Application. *Coatings* **2021**, *11*, 1528. https://doi.org/10.3390/coatings11121528.
49. Bernal, R.A.; Coradin, V.; Camargos, J.; Costa, C.; Pissarra, J. Wood Anatomy of Lecythidaceae Species Called "Tauari." *IAWA J.* **2011**, *32*, 97–112. https://doi.org/10.1163/22941932-90000046.
50. dos Santos, J.X.; Vieira, H.C.; da Silva, E.L.; de Muñiz, G.I.B.; Reis, A.R.S.; Nisgoski, S. Anatomical Characterization of Wood Marketed as "Tauari"(Lecythidaceae) in Pará State, Brazil. *Floresta* **2020**, *50*, 1421–1429. https://doi.org/10.5380/rf.v50i3.59399.
51. Santos, W.L.F.; Silva, A.J.P.d.; Cabral, A.A.; Mercury, J.M.R. Particleboard Manufactured from Tauari (*Couratari oblongifolia*) Wood Waste Using Castor Oil Based Polyurethane Resin. *Mat. Res.* **2014**, *17*, 657–663. https://doi.org/10.1590/S1516-14392014005000013.
52. Procópio, L.C.; Secco, R.d.S. The importance of botanical identification in forest inventories: The example of "tauari"—*Couratari* spp. and *Cariniana* spp., Lecythidaceae—In two timber areas of the State of Pará. *Acta Amaz.* **2008**, *38*, 31–44. https://doi.org/10.1590/S0044-59672008000100005.
53. Procópio, L.C.; Gayot, M.; Sist, P.; Ferraz, I.D. " Tauari" Species (Lecythidaceae) in Non-Flooded Amazon Forest: Patterns of Geographic Distribution, Abundance, and Implications for Conservation. *Acta Bot. Bras.* **2010**, *24*, 883–897.
54. Bozi, L.D.; Mascarenhas, A.R.P.; de Melo, R.R. Variação radial da densidade e estabilidade dimensional da madeira de tauari (*Couratari oblongifolia* Ducke & R. Knuth.). *Rev. Agroecossistemas* **2021**, *13*, 1–15. https://doi.org/10.18542/ragros.v13i2.7614.
55. Okino, E.Y.A.; Pastore, T.C.M.; Camargos, J.A.A.; Coradin, V.T.R.; Teixeira, D.E.; Santana, M.A.E.; Fagg, C.W. Accelerated Laboratory Test of Three Amazonian Wood Species Called Tauari, Exposed to White-and Brown-Rot Fungi and Color Response According to CIE L* A* B* System. *Ciênc. Florest.* **2015**, *25*, 581–593.
56. Orisaleye, J.I.; Ogundare, A.A.; Abiodun, Y.O.; Oyekeye, M.O.; Adefuye, O.A.; Ojolo, S.J.; Owoeye, O.E. An Investigation of the Effects of Manufacturing Parameters on Properties of Binderless Boards Produced from Abura (*Mitragyna ciliata*) Sawdust. *Int. J. Integr. Eng.* **2023**, *15*, 89–99.
57. Löfstrand, S.D.; Krüger, Å.; Razafimandimbison, S.G.; Bremer, B. Phylogeny and Generic Delimitations in the Sister Tribes Hymenodictyeae and Naucleeae (Rubiaceae). *Syst. Bot.* **2014**, *39*, 304–315. https://doi.org/10.1600/036364414X678116.
58. Wilson, U.N.; Adedeji, A.A.; Afolayan, J.O.; Mohammed, I.S.; Sani, J.E.; Alomaja, J.A.; Yoro, K.O. Reliability-Based Investigation on the Compressive Strength of Commonly Used Nigerian Timber Species. *Malays. J. Civ. Eng.* **2022**, *3*, 1–10. https://doi.org/10.11113/mjce.v34.17136.
59. Orisaleye, J.I.; Jekayinfa, S.O.; Ogundare, A.A.; Shittu, M.R.; Akinola, O.O.; Odesanya, K.O. Effects of Process Variables on Physico-Mechanical Properties of Abura (*Mitrogyna ciliata*) Sawdust Briquettes. *Biomass* **2024**, *4*, 671–686. https://doi.org/10.3390/biomass4030037.
60. Wédjangnon, A.A.; Sourou Kuiga, N.B.; Houêtchégnon, T.; Ouinsavi, C.A.I.N. Spatial Distribution and Interspecific Association Patterns between *Mansonia altissima* A. Chev., *Ceiba pentandra* (L.) Gaertn and *Triplochiton scleroxylon* K. Schum. in a Moist Semi-Deciduous Forest. *Ann. For. Sci.* **2020**, *77*, 6. https://doi.org/10.1007/s13595-019-0913-0.
61. Jayeola, A.; Aworinde, D.O.; Folorunso, A.E. Use of Wood Characters in the Identification of Selected Timber Species in Nigeria. *Not. Bot. Hort. Agrobot. Cluj.* **2009**, *37*, 28–32.
62. Ojo, A.R.; Ogutuga, S.O.; Aguda, L.O. Correlation between Dry Density and Shrinkage in Eight Tropical Hardwood Species: Zveza Med Gostoto in Krčenjem Lesa Osmih Tropskih Vrst. *Les/Wood* **2022**, *71*, 31–44. https://doi.org/10.26614/les-wood.2022.v71n02a02.
63. Makomra, V.; Oum Lissouck, R.; Pommier, R.; Ngoc, A.P.; Breysse, D.; Denaud, L.; Ayina Ohandja, L.M. Analysis of Drying Stresses in Green-Glued Plywood of Bete (*Mansonia altissima*) Specie. *J. Wood Sci.* **2020**, *66*, 70. https://doi.org/10.1186/s10086-020-01911-1.

64. Adeniyi, I.M.; Aina, K.S.; Akinlabi, F.M.; Odozie, E.C. Stem Fibres in Some Nigerian Wood Species. *Biol. Environ. Sci. J. Trop.* **2025**, *22*, 84–95. https://doi.org/10.4314/bestj.v22i1.10.
65. Adetayo, O.A.; Dahunsi, B.I. Variations of Density and Compressive Strength Before and After Charring of Some Selected Construction Timber Species of South-Western Nigeria. *Fuoye J. Eng. Technol.* **2017**, *2*, 43–46.
66. N'Guessan, J.L.L.; Niamké, B.F.; Ouattara, H.A.A.; Bley-Atse, B.A.; Ahoke, M.E.M.F.; Yao, N.J.C.; Amusant, N. Chemical Characterisation and Durability Enhancement of Kapok Wood Using Ivorian Plant Extracts. *Wood Mater. Sci. Eng.* **2026**, 1–15. https://doi.org/10.1080/17480272.2026.2632775.
67. Kozakiewicz, P.; Laskowska, A.; Ciolek, S. A Study of Selected Features of Shan Tong Variety of Plantation Paulownia and Its Wood Properties. *Ann. Wars. Univ. Life Sci. SGGW For. Wood Technol.* **2020**, *111*, 116–123. https://doi.org/10.5604/01.3001.0014.6904.
68. Barbu, M.C.; Burešova, K.; Tudor, E.M.; Sepperer, T. Exploring Paulownia as a Sustainable Alternative to Balsa in Plywood Manufacturing. *Forests* **2025**, *16*, 1436. https://doi.org/10.3390/f16091436.
69. Barbu, M.C.; Radauer, H.; Petutschnigg, A.; Tudor, E.M.; Kathriner, M. Lightweight Solid Wood Panels Made of Paulownia Plantation Wood. *Appl. Sci.* **2023**, *13*, 11234. https://doi.org/10.3390/app132011234.
70. Jakubowski, M. Cultivation Potential and Uses of Paulownia Wood: A Review. *Forests* **2022**, *13*, 668. https://doi.org/10.3390/f13050668.
71. Tomczak, K.; Mania, P.; Jakubowski, M.; Tomczak, A. Radial Variability of Selected Physical and Mechanical Parameters of Juvenile Paulownia Wood from Extensive Cultivation in Central Europe—Case Study. *Materials* **2023**, *16*, 2615. https://doi.org/10.3390/ma16072615.
72. Kulak, P.; Komorowicz, M.; Lachowicz, H. Fibre Morphological Characteristics, Chemical Composition and Fuel Properties of Paulownia COTEVISA-2 Wood. *Eur. J. Wood Wood Prod.* **2024**, *82*, 1605–1614. https://doi.org/10.1007/s00107-024-02108-9.
73. Jo, J.I.; Purusatama, B.D.; Kim, N.H. Qualitative and Quantitative Anatomical Characteristics and Radial Variation of Major Cell Components in *Paulownia tomentosa* Wood Grown in Korea. *Bioresources* **2024**, *19*, 2466. https://doi.org/10.15376/biores.19.2.2466-2479.
74. Nocetti, M.; Aminti, G.; Brunetti, M.; Palanti, S.; Stefanini, F.M.; Goli, G. Natural and Thermally Modified Paulownia Wood from Northern Italy Plantations: Sawing Yield, Sawn-Timber Quality, Properties and Durability. *Wood Mater. Sci. Eng.* **2026**, *21*, 1115–1124. https://doi.org/10.1080/17480272.2025.2469712.
75. Barbu, M.C.; Buresova, K.; Tudor, E.M.; Petutschnigg, A. Physical and Mechanical Properties of *Paulownia tomentosa* x Elongata Sawn Wood from Spanish, Bulgarian and Serbian Plantations. *Forests* **2022**, *13*, 1543. https://doi.org/10.3390/f13101543.
76. Ahmed, O.I.; Ibrahim, M.M.; Hasan, O.A.; Zainulabdeen, I.H. Study of Some Physical And Mechanical Characteristics of *Paulownia tomentosa* S. Wood Planted in Northern Iraq. *Anbar J. Agric. Sci.* **2025**, *23*, 162–172. https://doi.org/10.32649/ajas.2025.186588.
77. Komán, S. Quality Characteristics of the Selected Variant of *Paulownia tomentosa* (Robust4) Wood Cultivated in Hungary. *Maderas. Cienc. Tecnol.* **2023**, *25*, 1–6. https://doi.org/10.4067/s0718-221x2023000100401.
78. Sedlar, T.; Šefc, B.; Drvodelić, D.; Jambreković, B.; Kučinić, M.; Ištok, I. Physical Properties of Juvenile Wood of Two Paulownia Hybrids. *Drv. Ind.* **2020**, *71*, 179–184. https://doi.org/10.5552/drvind.2020.1964.
79. Broda, M.; Popescu, C.-M.; Poszwa, K.; Roszyk, E. How Thermal Treatment Affects the Chemical Composition and the Physical, Mechanical and Swelling Properties of Scots Pine Juvenile and Mature Wood. *Wood Sci. Technol.* **2024**, *58*, 1153–1180. https://doi.org/10.1007/s00226-024-01561-2.
80. *ISO 13061-2*; Physical and Mechanical Properties of Wood—Test Methods for Small Clear Wood Specimens—Part 2: Determination of Density for Physical and Mechanical Tests. International Organization for Standardization: Geneva, Switzerland, 2014.
81. Molinski, W.; Raczkowski, J. Ciśnienie pęcznienia drewna zmodyfikowanego polistyrenem. *Zesz. Probl. Postępów Nauk. Rol.* **1980**, *231*, 89–101.
82. Roszyk, E.; Kropaczewski, R.; Mania, P.; Broda, M. Swelling Behaviour of Bamboo (*Phyllostachys pubescens*). *Forests* **2024**, *15*, 118. https://doi.org/10.3390/f15010118.
83. Rybarczyk, W.; Ganowicz, R. A Theoretical Description of the Swelling Pressure of Wood. *Wood Sci. Technol.* **1974**, *8*, 233–241. https://doi.org/10.1007/BF00352027.
84. Huč, S.; Hozjan, T.; Svensson, S. Rheological Behavior of Wood in Stress Relaxation under Compression. *Wood Sci. Technol.* **2018**, *52*, 793–808. https://doi.org/10.1007/s00226-018-0993-2.

85. Akter, S.T.; Binder, E.; Bader, T.K. Moisture and Short-Term Time-Dependent Behavior of Norway Spruce Clear Wood under Compression Perpendicular to the Grain and Rolling Shear. *Wood Mater. Sci. Eng.* **2023**, *18*, 580–593. https://doi.org/10.1080/17480272.2022.2056715.
86. Wagenführ, R.; Wagenführ, A. *Holzatlas*; Carl Hanser Verlag GmbH Co KG: München, Germany, 2021.
87. Dimou, V.; Boufidou, E.; Kitikidou, K. Variation in Basic Density of *Paulownia tomentosa* along Axial and Radial Direction in Nurseries in Greece. *Int. Wood Prod. J.* **2025**, *16*, 148–156. https://doi.org/10.1177/20426445251332422.
88. Barbu, M.C.; Tudor, E.M.; Buresova, K.; Petutschnigg, A. Assessment of Physical and Mechanical Properties Considering the Stem Height and Cross-Section of *Paulownia tomentosa* (Thunb.) Steud. *x Elongata* (S.Y.Hu) Wood. *Forests* **2023**, *14*, 589. https://doi.org/10.3390/f14030589.
89. Esteves, B.; Aires, P.; Sen, U.; Gomes, M.D.G.; Guiné, R.P.F.; Domingos, I.; Ferreira, J.; Viana, H.; Cruz-Lopes, L.P. Particleboard Production from *Paulownia tomentosa* (Thunb.) Steud. Grown in Portugal. *Polymers* **2023**, *15*, 1158. https://doi.org/10.3390/polym15051158.
90. Esteves, B.; Cruz-Lopes, L.; Viana, H.; Ferreira, J.; Domingos, I.; Nunes, L.J.R. The Influence of Age on the Wood Properties of *Paulownia tomentosa* (Thunb.) Steud. *Forests* **2022**, *13*, 700. https://doi.org/10.3390/f13050700.
91. Chauhan, S.; Sethy, A. Differences in Dynamic Modulus of Elasticity Determined by Three Vibration Methods and Their Relationship with Static Modulus of Elasticity. *Maderas. Cienc. Tecnol.* **2016**, *18*, 373–382. https://doi.org/10.4067/S0718-221X2016005000034.
92. Baar, J.; Tippner, J.; Rademacher, P. Prediction of Mechanical Properties—Modulus of Rupture and Modulus of Elasticity—Of Five Tropical Species by Nondestructive Methods. *Maderas. Cienc. Tecnol.* **2015**, *17*, 239–252. https://doi.org/10.4067/S0718-221X2015005000023.
93. Mascarenhas, A.R.P.; de Melo, R.R.; Pimenta, A.S.; Stangerlin, D.M.; Corrêa, F.L.D.O.; Sccoti, M.S.V.; Paula, E.A.D.O. Ultrasound to Estimate the Physical-Mechanical Properties of Tropical Wood Species Grown in an Agroforestry System. *Holzforschung* **2021**, *75*, 879–891. https://doi.org/10.1515/hf-2020-0249.
94. Yang, J.L.; Evans, R. Prediction of MOE of Eucalypt Wood from Microfibril Angle and Density. *Holz Roh Werkst.* **2003**, *61*, 449–452. https://doi.org/10.1007/s00107-003-0424-3.
95. Hartwig-Nair, M.; Florisson, S.; Wohlert, M.; Gamstedt, E.K. Characterisation of Hygroelastic Properties of Compression and Opposite Wood Found in Branches of Norway Spruce. *Wood Sci. Technol.* **2024**, *58*, 887–906. https://doi.org/10.1007/s00226-024-01548-z.
96. Wang, W.; Sun, F.; Chen, Y.; Li, R.; Peng, H.; Lyu, J.; Zhan, T. Visualizing Intra-Ring Transverse Shrinking and Swelling of Chinese Fir. *Holzforschung* **2025**, *79*, 383–391. https://doi.org/10.1515/hf-2025-0034.
97. Ahmed, S.A.; Chun, S.K.; Miller, R.B.; Chong, S.H.; Kim, A.J. Liquid Penetration in Different Cells of Two Hardwood Species. *J. Wood Sci.* **2011**, *57*, 179–188. https://doi.org/10.1007/s10086-010-1168-4.
98. Jakes, J.E.; Hunt, C.G.; Zelinka, S.L.; Ciesielski, P.N.; Plaza, N.Z. Effects of Moisture on Diffusion in Unmodified Wood Cell Walls: A Phenomenological Polymer Science Approach. *Forests* **2019**, *10*, 1084. https://doi.org/10.3390/f10121084.
99. Peng, H.; Lu, J.; Jiang, J.; Cao, J. Longitudinal Mechano-Sorptive Creep Behavior of Chinese Fir in Tension during Moisture Adsorption Processes. *Materials* **2017**, *10*, 931. https://doi.org/10.3390/ma10080931.
100. O'Ceallaigh, C.; Sikora, K.; McPolin, D.; Harte, A.M. The Mechano-Sorptive Creep Behaviour of Basalt FRP Reinforced Timber Elements in a Variable Climate. *Eng. Struct.* **2019**, *200*, 109702. https://doi.org/10.1016/j.engstruct.2019.109702.
101. Kanno, K. Swelling Stress of Wood under Different Restraints. II. Relations between Swelling Stress and Several Properties of Wood. *J. Jpn. Wood Res. Soc./Mokuzai Gakkaishi* **1977**, *23*, 419–426.
102. de Borst, K.; Bader, T.K.; Wikete, C. Microstructure–Stiffness Relationships of Ten European and Tropical Hardwood Species. *J. Struct. Biol.* **2012**, *177*, 532–542. https://doi.org/10.1016/j.jsb.2011.10.010.
103. Kollmann, F.F.; Côté, W.A., Jr. *Principles of Wood Science and Technology. Vol. I. Solid Wood*; Springer: Berlin/Heidelberg, Germany, 1968.
104. Missanjo, E.; Matsumura, J. Wood Density and Mechanical Properties of Pinus Kesiya Royle Ex Gordon in Malawi. *Forests* **2016**, *7*, 135. https://doi.org/10.3390/f7070135.
105. Sonderegger, W.; Mandallaz, D.; Niemz, P. An Investigation of the Influence of Selected Factors on the Properties of Spruce Wood. *Wood Sci. Technol.* **2008**, *42*, 281–298. https://doi.org/10.1007/s00226-007-0173-2.
106. Qian, J.; Yue, K.; Li, X.; Pu, Y.; Chen, K.; Wu, P.; Zhang, Z. Strength Grading of Full-Scale Chinese Fast-Growing Poplar Wood for Structural Building Applications. *Forests* **2024**, *15*, 1602. https://doi.org/10.3390/f15091602.

107. Simo-Tagne, M.; Rémond, R.; Rogaume, Y.; Zoulalian, A.; Perré, P. Characterization of Sorption Behavior and Mass Transfer Properties of Four Central Africa Tropical Woods: Ayous, Sapele, Frake, Lotofa. *Maderas. Cienc. Tecnol.* **2016**, *18*, 207–226. https://doi.org/10.4067/S0718-221X2016005000020.
108. de Borst, K.; Bader, T.K. Structure–Function Relationships in Hardwood—Insight from Micromechanical Modelling. *J. Theor. Biol.* **2014**, *345*, 78–91. https://doi.org/10.1016/j.jtbi.2013.12.013.
109. Thybring, E.E.; Fredriksson, M.; Zelinka, S.L.; Glass, S.V. Water in Wood: A Review of Current Understanding and Knowledge Gaps. *Forests* **2022**, *13*, 2051. https://doi.org/10.3390/f13122051.

Disclaimer/Publisher's Note: The statements, opinions and data contained in all publications are solely those of the individual author(s) and contributor(s) and not of MDPI and/or the editor(s). MDPI and/or the editor(s) disclaim responsibility for any injury to people or property resulting from any ideas, methods, instructions or products referred to in the content.